Absolute total electronically elastic differential e^--H_2 scattering cross-section measurements from 1 to 19 eV

J. Furst, M. Mahgerefteh, and D. E. Golden
Department of Physics and Astronomy, University of Oklahoma, Norman, Oklahoma 73019
(Received 7 May 1984)

Absolute e^--H_2 total electronically elastic differential scattering cross sections have been determined from relative scattered-electron angular distribution measurements in the energy range from 1 to 19 eV by comparison to absolute e^--He elastic differential scattering cross sections measured in the same apparatus. Integrated total cross sections have been determined as well. Absolute differences as large as 50% between the present results and some previous results have been found, although the agreement as to shape is quite good in many cases. The present results are generally in excellent agreement with recent full rovibrational laboratory-frame close-coupling calculations.

I. INTRODUCTION

The scattering of electrons from simple ground-state target molecules resulting in elastic scattering, and/or vibrational, and/or rotational excitation has been the subject of a rather considerable effort in recent years. For a detailed review of the subject, the reader is referred to a number of excellent reviews as well as the references contained therein.[1–6] Nevertheless, although H_2 is the simplest molecule to deal with, one cannot get very far into the literature without discovering very serious discrepancies between experiments, between calculations, and between experiments and calculations.

The first accurate electronically elastic total differential cross-section (DCS) measurements in the energy range 0.3—15 eV were made by Linder and Schmidt,[7] who put their results on an absolute basis by normalizing to the total cross-section results of Golden *et al.*[8] More recently, additional absolute total electronically elastic DCS have been measured by Srivastava *et al.*[9] and Shyn and Sharp.[10] In some cases these measurements disagree with each other by as much as a factor of 2.

In our laboratory we have begun a comprehensive program which uses a pulsed-electron-beam time-of-flight technique to determine accurate relative differential cross sections for these quantities. In this work we present the results of total electronically elastic differential and total integrated e^--H_2 scattering sections in the energy range from 1 to 19 eV.

II. APPARATUS AND PROCEDURE

The apparatus and procedure used in this work will only briefly be described here, since it is similar to that described in more detail previously.[11] A pulsed electron gun is crossfired with a well-collimated (skimmed and differentially pumped) neutral beam. The arrival-time spectrum of scattered electrons is studied as a function of scattering angle while a stationary detector monitors a scattered signal which is proportional to the product of electron-beam current and background-gas density. This latter signal is used to normalize the signal from the rotating electron detector. The normalized scattered-electron signal is also studied as a function of electron scattering angle when the neutral beam is off and the chamber is flooded to the same background pressure as when the neutral beam is on. The second signal is subtracted from the first at each angle studied to determine relative differential cross sections. The relative differential cross section $d\sigma(E,\theta)/d\Omega$ at a particular electron energy E for scattering angles θ is determined from

$$d\sigma(E,\theta)/d\Omega = \frac{\mathring{R}(E,\theta)}{\mathring{S}(E,\theta)} - \frac{\mathring{R}'(E,\theta)}{\mathring{S}'(E,\theta)} , \quad (1)$$

where $\mathring{R}$ and $\mathring{S}$ are the scattering rates measured by the rotating and stationary detectors with the neutral beam on, while $\mathring{R}'$ and $\mathring{S}'$ are these scattering rates with the neutral beam off and the chamber flooded to the same background pressure. Throughout these measurements a grid in front of each detector was biased so that electrons which had excited an electronic level of H_2 were not detected.

A. Absolute cross-section determinations

The relative differential cross sections are placed on an absolute scale by comparison to measurements of absolute elastic e^--He scattering cross sections made in the same apparatus.[11] For this normalization, both He and H_2 relative differential cross-section measurements at 90° are made at each energy studied using the same neutral-beam driving pressure (measured by an MKS Baratron), background gas pressure, electron-beam current, voltages, etc.[12] In the normalization process the driving pressure in the gas reservoir should be sufficiently low so that the gas outflow is laminar. Under such conditions, a constant pressure in the gas reservoir together with a small rate of outflow is sufficient to give equal target beam densities for He and H_2 at the same gas reservoir pressure. This point has been discussed in detail by Srivastava *et al.*[9]

The absolute values of the differential cross sections previously determined in He at 2, 5, 12, and 19 eV at 90° together with their respective errors,[11] are given in Table I. Relative measurements made at these energies in H_2

TABLE I. Differential cross sections in He and H_2 from 1 to 19 eV determined in this work.

Energy (eV)	$\frac{d\sigma[\mathrm{He}(90°)]}{d\Omega}$ (Å^2/sr)	$\frac{d\sigma[\mathrm{H_2}(90°)]}{d\Omega} / \frac{d\sigma[\mathrm{He}(90°)]}{d\Omega}$	$\frac{d\sigma[\mathrm{H_2}(90°)]}{d\Omega}$ (Å^2/sr)	$\sigma(\mathrm{H_2})$ (Å^2)
1	0.470	2.23	1.05	14.2 ±13%
2	0.453±9%	2.16±8.8%	0.978±12.6%	15.7 ±13%
4	0.408	2.01	0.820	15.1 ±12%
5	0.381±7.7%	1.94±6.0%	0.739±9.8%	15.2 ±10%
6	0.372	1.87	0.696	13.25±9%
8	0.338	1.73	0.585	11.3 ±8%
10	0.307	1.59	0.488	10.2 ±8%
12	0.279±7%	1.46±2.2%	0.407±7.3%	9.8 ±9%
19	0.201±2%	1.08±2.9%	0.217±3.5%	6.8 ±10%

have been placed on an absolute scale by measuring the cross sections in H_2 relative to that in He at 90° for each energy. In this aspect of the work at least four determinations at each energy have been made. These relative values with their respective errors are also given in Table I.

The *s*-, *p*-, and *d*-wave phase shifts found at 2, 5, 12, and 19 eV in He have been fitted with effective range formulas to interpolate and extrapolate to the other energies given in Table I. The resulting phase shifts have been used to calculate the He cross sections at 90° given in Table I. The relative H_2-to-He cross-section ratios measured at 2, 5, 12 and 19 eV have been fitted with a third-order polynomial to obtain the values of this quantity given in Table I. The H_2 differential cross-section values at 90° given in Table I were obtained by multiplying the He cross sections by the H_2-to-He cross-section ratios at each energy. In this fashion, the relative angular distribution measurements at the other energies given in the table were placed on an absolute scale.

The absolute total differential cross sections were fitted with third-order polynomials and extrapolated to 0° and 180°. These fitted functions were integrated in order to obtain the integrated total cross sections $\sigma(E)$ also given in Table I.

B. Error analysis

In our previous work in He,[11] we have given errors which vary between about ±9% at 2 eV to ±2% at 19 eV. The errors in the relative cross sections in H_2 determined in this work vary from a maximum of ±8.8% at 2 eV to a minimum of about ±2.8% at 12 eV. These errors have been combined to determine the errors in the H_2 absolute cross sections given in Table I. The errors in the integrated total cross sections given in the table have been determined by the differences introduced into the integrated total cross sections due to differences in the possible extrapolations.

III. RESULTS

Total differential cross sections measured at 1, 2, 4, 5, 6, 8, 10, 12, and 19 eV are plotted in Figs. 1—9 together

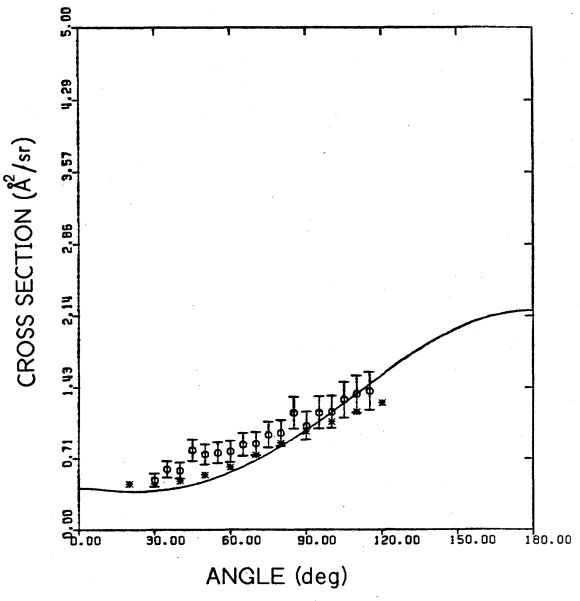

FIG. 1. Differential cross section at 1 eV. ○, present results; ——, Morrison *et al.*; *, Linder and Schmidt.

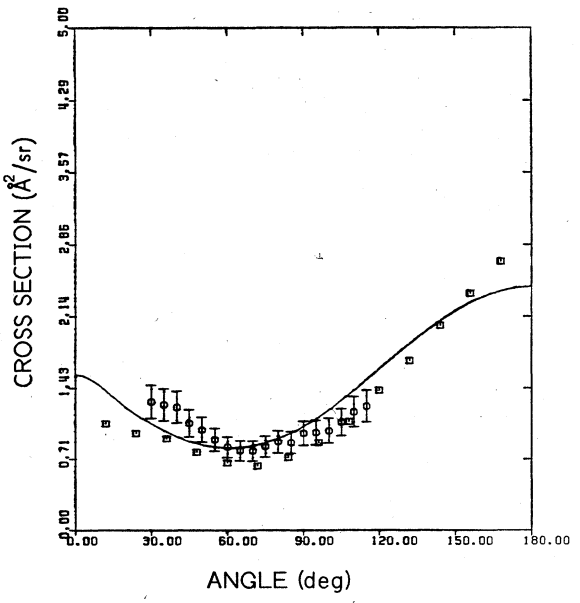

FIG. 2. Differential cross section at 2 eV. ○, present results; ——, Morrison *et al.*; □, Shyn and Sharp.

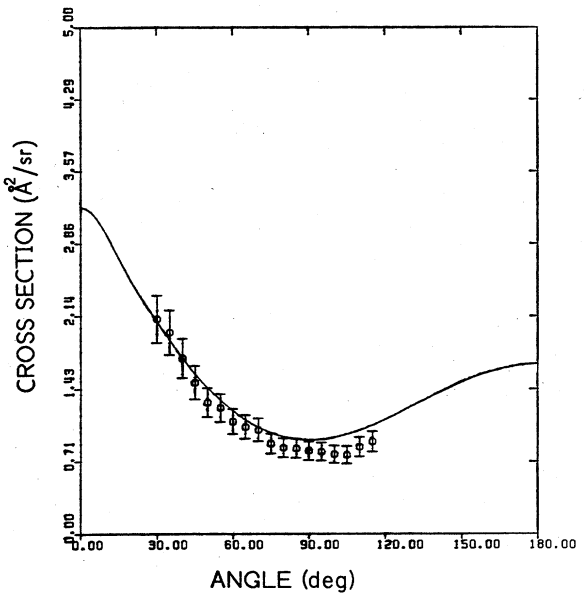

FIG. 3. Differential cross section at 4 eV. ○, present results; ——, Morrison *et al.*

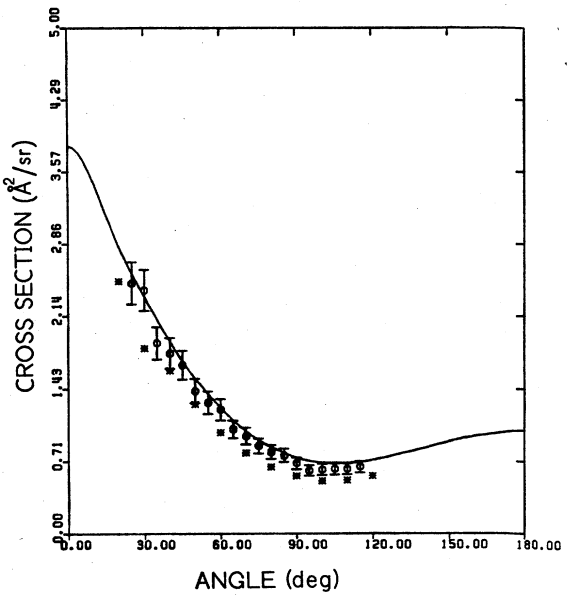

FIG. 5. Differential cross section at 6 eV. ○, present results; ——, Morrison *et al.*; ∗, Linder and Schmidt.

with the previous experimental results of Linder and Schmidt,[7] Srivastava *et al.*,[9] Trajmar *et al.*,[15] and Shyn and Sharp,[10] and the calculations of Morrison *et al.*[13] The absolute total differential cross sections found in the present work are summarized in Table II.

The measurements of Srivastava *et al.*[9] (shown on the plots) have been renormalized to the He results of Register *et al.*[14,15] The agreement between the present measurements and the recent full rovibrational laboratory-frame close-coupling calculations of Morrison *et al.*[13] is excellent over the complete energy range of overlap. In general, the present results are above those of Srivastava *et al.*[9] and Trajmar *et al.*[15] in the forward direction (~25% at 30° and 10 eV) and in agreement with them in the backward direction. In contrast, the present results are generally in agreement with those of Shyn and Sharp[10]

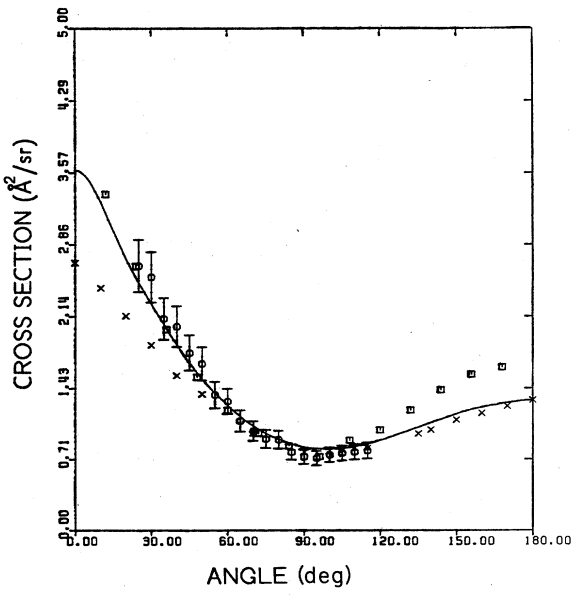

FIG. 4. Differential cross section at 5 eV. ○, present results; ——, Morrison *et al.*; ×, Srivastava *et al.* and Trajmar *et al.*; □, Shyn and Sharp.

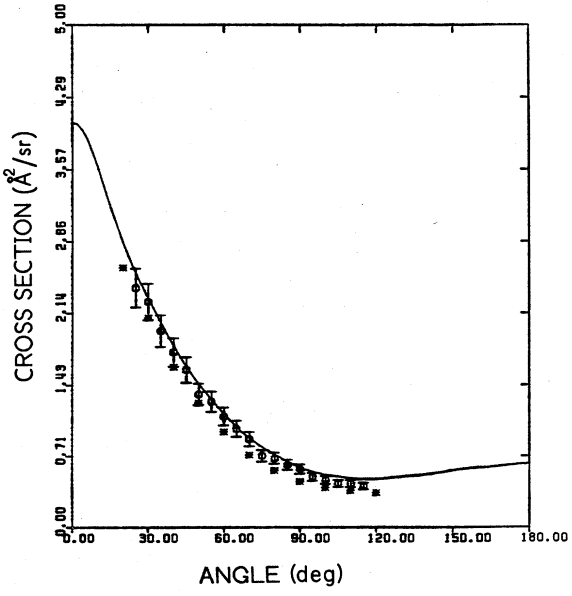

FIG. 6. Differential cross section at 8 eV. ○, present results; ——, Morrison *et al.*; ∗, Linder and Schmidt.

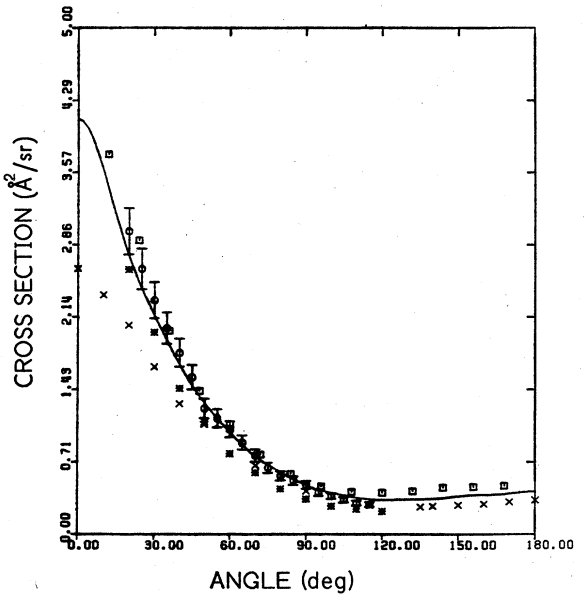

FIG. 7. Differential cross section at 10 eV. ○, present results; ——, Morrison *et al.*; ∗, Linder and Schmidt; ×, Srivastava *et al.* and Trajmar *et al.*; □, Shyn and Sharp.

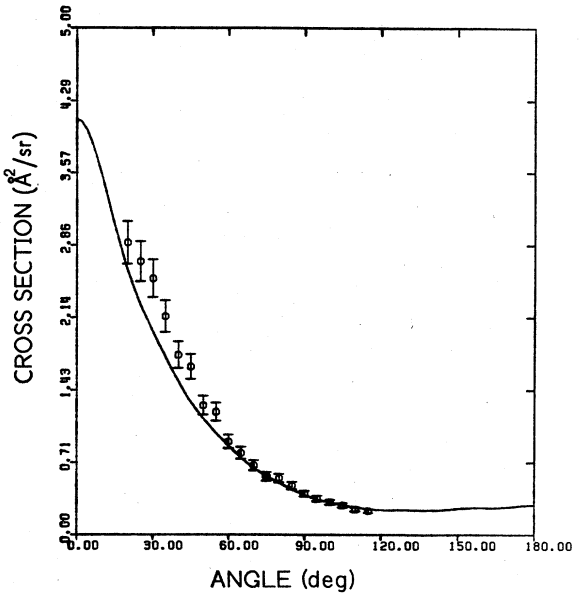

FIG. 8. Differential cross section at 12 eV. ○, present results; ——, Morrison *et al.*

in the forward direction but below them in the backward direction (~50% at 115° and 10 eV). The present results are generally higher than those of Linder and Schmidt[7] (~25% at 10 eV) although the two sets of results are very similar in shape and become closer in absolute magnitude as one goes to lower energies.

The integrated total cross sections found in this work are presented in Fig. 10 together with the previous direct determinations of Dalba *et al.*[16] and Jones,[17] the integrated total DCS measurements of Srivastava *et al.*,[9] Trajmar

TABLE II. Elastic differential cross sections for H_2 in Å²/sr.

Scattering angle (deg)	Collision energy (eV)								
	1	2	4	5	6	8	10	12	19
20							2.99	3.53	2.84
25				2.65	2.47	2.40	2.62	3.10	2.61
30	0.498	1.30	2.12	2.54	2.40	2.26	2.31	2.66	2.26
35	0.606	1.27	1.98	2.12	1.88	1.97	2.03	2.30	1.81
40	0.594	1.24	1.73	2.04	1.78	1.76	1.79	1.91	1.38
45	0.798	1.08	1.49	1.78	1.66	1.58	1.55	1.76	1.12
50	0.756	1.02	1.30	1.67	1.05	1.33	1.24	1.40	0.910
55	0.773	0.913	1.24	1.36	1.29	1.24	1.15	1.26	0.785
60	0.786	0.838	1.11	1.30	1.22	1.11	1.04	0.994	0.630
65	0.855	0.802	1.05	1.10	1.03	0.991	0.909	0.847	0.507
70	0.864	0.799	1.02	0.997	0.963	0.886	0.779	0.710	0.393
75	0.955	0.842	0.890	0.919	0.866	0.719	0.657	0.610	0.319
80	0.971	0.893	0.849	0.910	0.806	0.694	0.577	0.540	0.256
85	1.18	0.883	0.843	0.786	0.773	0.627	0.532	0.485	0.226
90	1.05	0.978	0.820	0.739	0.696	0.585	0.488	0.407	0.217
95	1.18	0.985	0.812	0.726	0.623	0.509	0.410	0.354	0.170
100	1.19	1.00	0.784	0.758	0.634	0.475	0.378	0.315	0.144
105	1.31	1.09	0.777	0.775	0.638	0.441	0.342	0.295	0.126
110	1.36	1.19	0.858	0.786	0.641	0.440	0.309	0.259	0.122
115	1.40	1.25	0.910	0.799	0.659	0.414	0.295	0.260	0.122

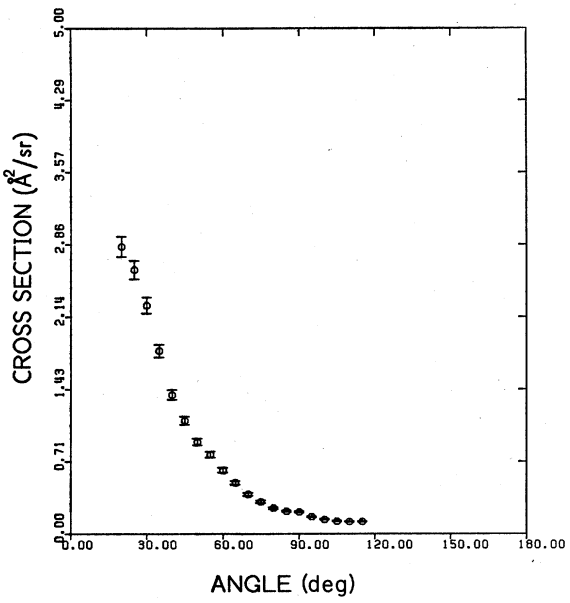

FIG. 9. Differential cross section at 19 eV. ○, present results.

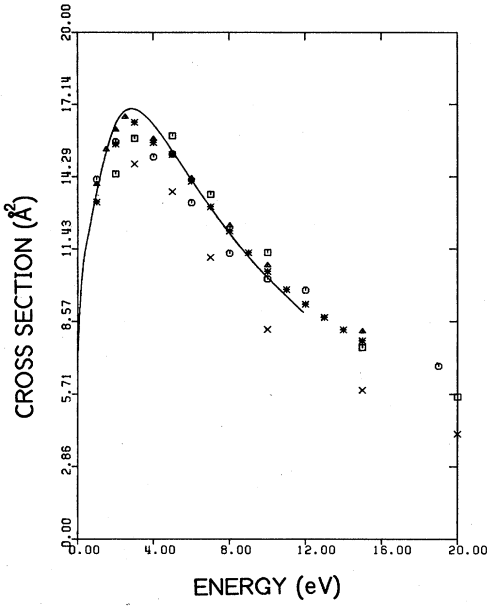

FIG. 10. Integrated total cross section in H_2. ○, present results; ——, Morrison *et al.*; ×, Srivastava *et al.* and Trajmar *et al.*; □, Shyn and Sharp; △, Dalba *et al.*; ✱, Jones.

et al.,[15] and Shyn and Sharp,[10] as well as the calculations of Morrison *et al.*[13] The present results agree best with the older direct measurements of Golden *et al.*,[8] the other two direct measurements, and the recent calculation shown on the plot.

ACKNOWLEDGMENT

This work was supported by the Office of Basic Energy Sciences, U.S. Department of Energy.

[1]A. V. Phelps, Rev. Mod. Phys. **40**, 399 (1968).
[2]H. S. W. Massey, E. H. S. Burhop, and H. B. Gilbody, *Electronic and Ionic Impact Phenomena* (Oxford University, Oxford, England, 1969).
[3]D. E. Golden, N. F. Lane, A. Temkin, and E. Gerjuoy, Rev. Mod. Phys. **43**, 462 (1971).
[4]G. J. Schulz, Rev. Mod. Phys. **45**, 423 (1973).
[5]D. E. Golden, Adv. At. Mol. Phys. **14**, 1 (1978).
[6]N. F. Lane, Rev. Mod. Phys. **52**, 29 (1980).
[7]F. Linder and M. Schmidt, Z. Naturforsch. **26a**, 1603 (1971).
[8]D. E. Golden, H. W. Bandel, and J. A. Salerno, Phys. Rev. **146**, 40 (1966).
[9]S. K. Srivastava, A. Chutjian, and S. Trajmar, J. Chem. Phys. **63**, 2659 (1975).
[10]T. W. Shyn and W. E. Sharp, Phys. Rev. A **24**, 1734 (1981).
[11]D. E. Golden, J. Furst, and M. Mahgerefteh, Phys. Rev. A **30**, 1247 (1984).
[12]The accelerating voltage is slightly adjusted when changing gases in order to keep the electron energy the same.
[13]M. Morrison, A. Feldt, and B. Saha (private communication).
[14]D. F. Register, S. Trajmar, and S. K. Srivastava, Phys. Rev. A **21**, 1134 (1980).
[15]See, for example, S. Trajmar, D. F. Register, and A. Chutjian, Phys. Rep. **97**, 219 (1983).
[16]G. Dalba, P. Fornasini, I. Lazzizzera, G. Ranieri, and A. Zecca, J. Phys. B **13**, 2839 (1980).
[17]R. K. Jones (private communication).